The Astrophysical Journal Letters, 903:L35 (7pp), 2020 November 10 https://doi.org/10.3847/2041-8213/abc25c

Methanimine as a Key Precursor of Imines in the Interstellar Medium: The Case of Propargylimine

Jacopo Lupi[1], Cristina Puzzarini[2], and Vincenzo Barone[1]
[1] Scuola Normale Superiore, Piazza dei Cavalieri 7, Pisa, I-56126, Italy; vincenzo.barone@sns.it
[2] Department of Chemistry "Giacomo Ciamician," University of Bologna, Via F. Selmi 2, Bologna, I-40126, Italy; cristina.puzzarini@unibo.it
Received 2020 August 11; revised 2020 October 5; accepted 2020 October 17; published 2020 November 9

Abstract

A gas-phase formation route is proposed for the recently detected propargylimine molecule. In analogy to other imines, such as cyanomethanimine, the addition of a reactive radical (C_2H in the present case) to methanimine (CH_2NH) leads to reaction channels open also in the harsh conditions of the interstellar medium. Three possible isomers can be formed in the $CH_2NH + C_2H$ reaction: Z- and E-propargylimine (Z-,E-PGIM) as well as N-ethynylmethanimine (N-EMIM). For both PGIM species, the computed global rate coefficient is nearly constant in the 20–300 K temperature range, and of the order of 2–3 $\times$ 10^{-10} cm^3 $molecule^{-1}$ s^{-1}, while that for N-EMIM is about two orders of magnitude smaller. Assuming equal destruction rates for the two isomers, these results imply an abundance ratio for PGIM of [Z]/[E] $\sim$ 1.5, which is only slightly underestimated with respect to the observational datum.

Unified Astronomy Thesaurus concepts: Interstellar molecules (849); Interstellar medium (847); Interstellar abundances (832); Astrochemistry (75)

1. Introduction

Currently, the number of molecules detected in the interstellar medium (ISM) thanks to their rotational signatures far exceeds 200 (McGuire 2018). Among them, more than 70 species belong to the class of the so-called interstellar complex organic molecules (iCOMs), namely molecules containing at least one carbon atom and a total of more than six atoms (Herbst & van Dishoeck 2009). Nitrogen-bearing iCOMs are particularly interesting because of their prebiotic character; indeed, they represent key intermediates toward the main building blocks of biomolecules, like amino acids and nucleobases. Within this class of iCOMs, six members of the imine family have been detected so far in the ISM, namely methanimine (CH_2NH, Godfrey et al. 1973; Dickens et al. 1997), ethanimine (CH_3CHNH, Loomis et al. 2013), ketenimine (CH_2CNH, Lovas et al. 2006), 3-imino-1,2-propadienylidene (CCCNH, Kawaguchi et al. 1992), C-cyanomethanimine (NCCHNH, Zaleski et al. 2013; Rivilla et al. 2018), and—very recently—Z-propargylimine (2-propyn-1-imine, HC≡C-CH=NH, Bizzocchi et al. 2020).

The main hypotheses on their formation mechanisms in astrophysical environments involve either tautomerization of simple nitriles (Lovas et al. 2006) or their partial hydrogenation on dust-grain surface (Theule et al. 2011; Krim et al. 2019). However, for C-cyanomethanimine, a gas-phase formation route has been recently proposed that involves addition of the cyano radical (CN) to methanimine (Vazart et al. 2015). It is thus quite natural to hypothesize that methanimine can play a role in the formation of other imines upon addition/elimination of reactive radicals already detected in the ISM, like CH_3, C_2H or OH. Indeed, the reaction of the hydroxyl radical with methanimine is proven to effectively lead to the formation of formamide in the gas phase (Vazart et al. 2016; Codella et al. 2017).

The focus of the present Letter is the possible formation pathway of propargylimine (PGIM), whose Z-isomer has been very recently identified in the quiescent G+0.693-0.027 molecular cloud with an estimated column density of 0.24 $\pm$ 0.02 $\times$ 10^{14} cm^{-2} (Bizzocchi et al. 2020). In the same study, an upper limit of 0.9 $\times$ 10^{-10} was retrieved for the fractional abundance (w.r.t. H_2) of the higher-energy E isomer (which means a column density $<$0.13 10^{14} cm^{-2}), which instead was not observed. After the spectroscopic characterization of this imine and its astronomical detection, Bizzocchi et al. (2020) put forward some speculations about feasible formation routes based on the relative abundances of a number of possible precursors in the G+0.693-0.027 molecular cloud. However, in spite of the detection of CH_2NH (Zeng et al. 2018), this has not been taken into consideration, notwithstanding the authors reported, among the others, a large fractional abundance for the ethynyl radical (C_2H, $^2\Sigma^+$), i.e., 3.91 $\times$ 10^{-8}.

Based on these premises, we decided to perform a state-of-the-art quantum-chemical (QC) characterization of the stationary points on the doublet reactive $C_2H + CH_2NH$ potential energy surface (PES) followed by kinetic computations in the framework of a master equation model rooted in generalized transition state estimates of the elementary reaction rates. From a theoretical point of view, the reactions between the ethynyl radical and several substrates have been recently investigated by state-of-the-art QC approaches (Bowman et al. 2020), but addition/elimination reactions with unsaturated substrates have not yet been explored.

2. Computational Methodology

The starting point for the study of the formation pathway of PGIM is the identification of the potential reactants and the analysis of the corresponding reactive PES, which implies the accurate characterization of all stationary points from both a structural and energetic point of view. This first step then requires to be completed by kinetic calculations. In the derivation of a feasible reaction mechanism, one has to take into account the extreme conditions of the ISM: low temperatures (10–100 K) and low number density (10–10^7 cm^{-3}). By translating density in

terms of pressure, a number density of 10^4 cm^{-3} corresponds to a pressure of 3.8×10^{-10} Pa ($\sim 3.8 \times 10^{-15}$ atm).

2.1. Reactive Potential Energy Surface

We have followed the general computational strategy validated in several recent studies (Baiano et al. 2020; Lupi et al. 2020; Puzzarini et al. 2020; Salta et al. 2020; Tonolo et al. 2020), which involves the following steps.

1. The stationary points have been located and characterized using the double-hybrid B2PLYP functional (Grimme 2006), combined with D3(BJ) corrections (to incorporate dispersion effects; Grimme et al. 2010, 2011) and in conjunction with the jun-cc-pVTZ "seasonal" basis set (Papajak et al. 2011).
2. Single-point energy calculations, at the B2PLYP-D3(BJ)/jun-cc-pVTZ geometries, have been performed by means of the so-called "cheap" composite scheme (ChS; Puzzarini & Barone 2011; Puzzarini et al. 2014), which starts from the coupled-cluster theory including single and double excitations augmented by a perturbative estimate of triples (CCSD(T); Raghavachari et al. 1989) in conjunction with a triple-zeta basis set (cc-pVTZ; Dunning 1989) and within the frozen-core (fc) approximation. To improve this level of theory, the ChS model considers the extrapolation to the complete basis set (CBS) limit and the effect of core-valence (CV) correlation using Møller-Plesset theory to second order (MP2; Møller & Plesset 1934). Concerning the former contribution, the fc-MP2 energy is extrapolated to the CBS limit using the n^{-3} expression (Helgaker et al. 1997) in conjunction with the cc-pVTZ and cc-pVQZ basis sets. The CV correlation correction is, instead, the difference between the MP2 energy evaluated correlating all electrons and that computed within the fc approximation, both in conjunction with the cc-pCVTZ basis set (Woon & Dunning 1995).
3. ChS energies have been combined with anharmonic zero-point energy (ZPE) corrections evaluated at the B2PLYP-D3(BJ)/jun-cc-pVTZ level within hybrid degeneracy-corrected second-order vibrational perturbation theory (HDCPT2; Bloino et al. 2012; Puzzarini et al. 2019).

All calculations have been performed with the Gaussian software (Frisch et al. 2016).

2.2. Kinetic Models

Global rate constants have been calculated by using a master equation (ME) approach based on ab initio transition state theory (AITSTME), thereby employing the MESS software as master equation solver (Georgievskii et al. 2013). For elementary reactions involving a transition state, rate constants have been computed using transition state theory (TST), while for barrierless elementary reactions, they have been evaluated by means of phase space theory (PST; Pechukas & Light 1965; Chesnavich 1986). The basic assumption of PST is that the interaction between two reacting fragments is isotropic (following a $\frac{C_6}{R^6}$ power law) and does not affect the internal fragment motions (Fernández-Ramos et al. 2006). This approximation is generally valid for low-temperature phenomena, as those occurring in the ISM. To be more precise, in order to obtain the C_6 parameter for the PST calculation, we performed a scan of the HCC-CH_2NH and HCC-$NHCH_2$ distances for the C- and N-end attack, respectively. Then, the corresponding minimum energy paths have been fitted to a $f(x) = f_0 - \frac{C_6}{x^6}$ function, thus obtaining a C_6 value of 131.96 $a_0{}^6 E_h$ for the former attack and of 180.59 $a_0{}^6 E_h$ for the latter. In all cases, tunneling has been accounted for using the Eckart model (Eckart 1930).

The rate constants of the overall reactions leading to the C_3H_3N imine isomers (namely, the E-,Z-PGIM species and N-ethynyl-methanimine, N-EMIM) have been evaluated in the 20–500 K temperature range. To model their temperature dependence, the rate constants at different temperatures have been fitted to a three-parameter modified Arrhenius equation, namely the Arrhenius–Kooij expression (Kooij 1893; Laidler 1996):

$$k(T) = A\left(\frac{T}{300}\right)^n \exp\left(-\frac{E}{RT}\right) \quad (1)$$

where A, n, and E are the fitting parameters, R being the universal gas constant.

3. Results and Discussion

3.1. Reactivity and Energetics

A recent re-investigation of the reaction channel starting from the attack of the cyano radical to the C-end of methanimine (Puzzarini & Barone 2020) has shown that, for all stationary points, the ChS model has a maximum absolute deviation of 3 kJ mol^{-1} and an average absolute deviation of 1.1 kJ mol^{-1} with respect to a reference composite scheme, which is able to reach sub-kJ accuracy energetics. These errors are much smaller than those issuing from widely employed composite schemes (e.g., CBS-QB3, Montgomery et al. 2000, or G4, Curtiss et al. 2007) and well sufficient for obtaining quantitative estimates of reaction rates and branching ratios (Baiano et al. 2020; Lupi et al. 2020; Puzzarini et al. 2020; Salta et al. 2020; Tonolo et al. 2020). On these grounds, we have performed a full characterization of the doublet PES for the addition-elimination reactions of both CN and CCH radicals to methanimine at the ChS level.

As far as the reaction mechanism is concerned, hydrogen abstraction could be competitive with addition/elimination (Bowman et al. 2020), but test computations showed that the former reaction channel is at least one order of magnitude slower than the latter one. As a consequence, only the addition/elimination reaction channel is analyzed in detail in the following. The reaction mechanism proposed in the present Letter for the formation of N-EMIM and the PGIM isomers is sketched in Figure 1 and the relative energies of all the stationary points, with respect to reactants, are collected in Table 1 together with the corresponding results for the CH_2NH+CN reaction. There are three possible initial adducts, corresponding to the attack of the ethynyl radical to the C or N ends and to the π-system of the imine double bond. However, the cyclic adduct resulting from the third option (CYCLO-1) is significantly less stable and easily interconverts to one of the corresponding open-chain minima (1Z or 1N). For both the CN and CCH radicals, the intermediate obtained upon attack to the N moiety is slightly more stable, but the reaction channels originating from it are ruled by transition states significantly less stable (albeit always submerged) than those ruling the corresponding channels issuing from 1Z or 1E. Noted is that

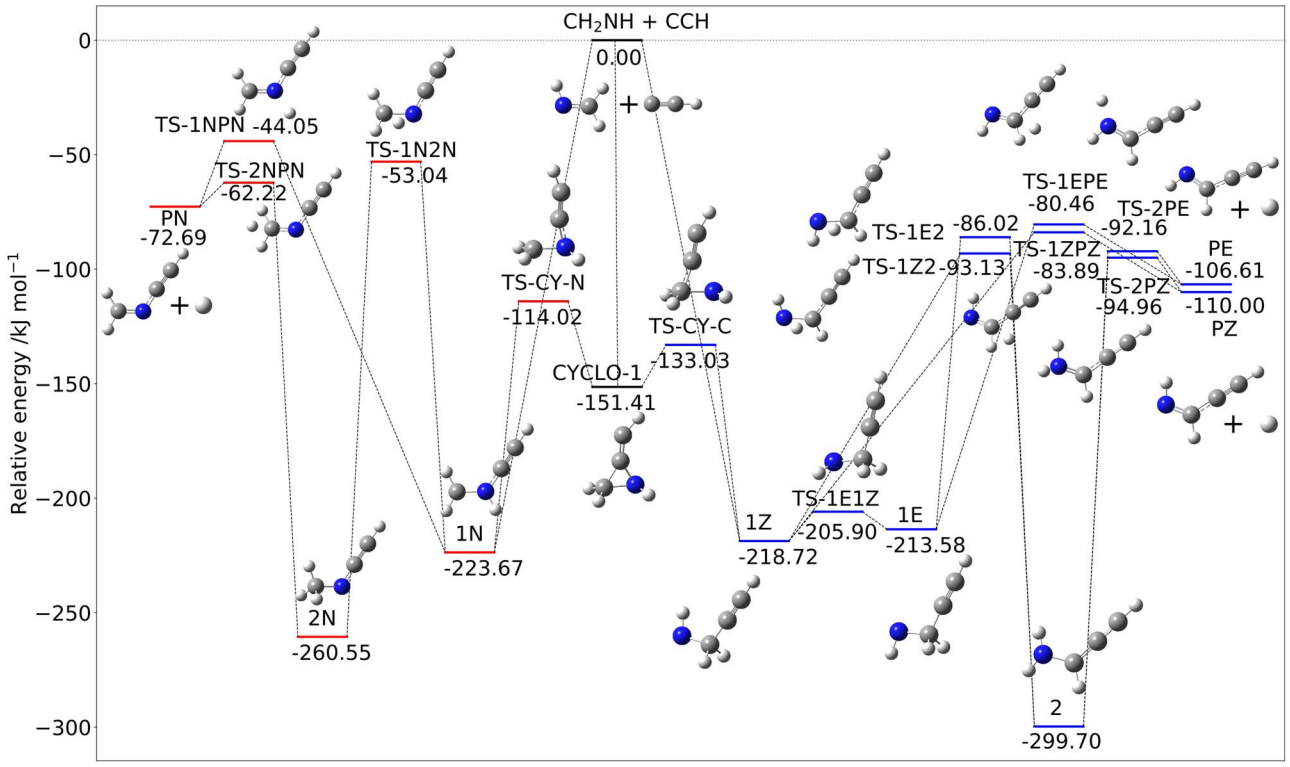

Figure 1. Formation route of N-EMIM and the PGIM isomers: ChS energies augmented by anharmonic B2PLYP-D3(BJ) ZPE corrections.

Table 1
ChS Relative Electronic Energies (ΔE_{el}) and Corresponding Standard Enthalpies at 0 K (ΔH_0°) for the Stationary Points of the CH_2NH+X Reaction

	X = C_2H		X = CN	
	ΔE_{el}	ΔH_0°	ΔE_{el}	ΔH_0°
CH_2NH + X	0.00	0.00	0.00	0.00
1Z	−229.36	−218.72	−203.59	−198.67
TS-1E1Z	−217.65	−205.90	−192.39	−183.24
1E	−225.75	−213.58	−201.48	−191.95
TS-1Z2	−96.36	−93.13	−63.55	−62.81
TS-1E2	−88.80	−86.02	−57.47	−57.18
2	−314.60	−299.70	−284.59	−271.29
TS-2PZ	−88.09	−94.96	−48.37	−58.27
TS-2PE	−84.99	−92.16	−46.22	−56.40
TS-1ZPZ	−77.81	−83.89	−40.62	−49.89
TS-1EPE	−73.86	−80.46	−37.97	−47.70
Z-IM + H (PZ)	−99.21	−110.00	−60.89	−74.73
E-IM + H (PE)	−95.40	−106.61	−58.55	−72.78
CYCLO-1	−167.50	−151.41	−108.93	−96.69
TS-CY-C	−144.35	−133.03	−97.62	−88.32
TS-CY-N	−122.80	−114.02	−88.77	−80.94
1N	−233.04	−223.67	−208.44	−201.33
TS-1N2N	−53.16	−53.04	−25.66	−27.16
2N	−272.23	−260.55	−223.19	−211.86
TS-2NPN	−52.98	−62.22	−22.76	−33.56
TS-1NPN	−35.54	−44.05	−3.85	−14.68
N-IM + H (PN)	−59.22	−72.69	−30.64	−45.80

Note. Values in kJ mol^{-1}.

the PES for the CH_2NH+CN reaction is, in any detail, analogous to that of the C_2H radical.

Starting from the very stable 1Z (or 1E) pre-reactive complex, one might observe a loss of the hydrogen radical, leading directly to the Z (or E) isomer of PGIM. This step has an exit barrier of about ∼135 (or ∼133) kJ mol^{-1}. On the other hand, considering the presence of the stabilizing C_2H moiety on the carbon atom, hydrogen migration might be observed in order to localize the unpaired electron on this atom. This migration occurs through the submerged transition state TS-1Z2 (TS-1E2 for the E-PGIM), which lies 125.6 kJ mol^{-1} above 1Z (127.6 kJ mol^{-1} above 1E for the E-route), thus forming the most stable intermediate of the whole PES, namely 2, which is nearly 300 kJ mol^{-1} below the reactants. Next, loss of hydrogen leads again to the Z (or E) form of PGIM through the submerged transition state TS-2PZ (TS-2PE), lying about 95 kJ mol^{-1} (92 kJ mol^{-1} for the E species) below the reactants (exit barrier of about 205 and 208 kJ mol^{-1}, respectively). The comparison with the analogous reaction paths for the gas-phase production of C-cyanomethanimine (Puzzarini & Barone 2020) shows that the formation of PGIM is characterized by greater exothermicity (−108 versus −60 kJ mol^{-1} for the average of Z and E isomers) and lower exit barriers (126 versus 140 kJ mol^{-1} for the average of TS-1Z2 and TS-1E2 and 206 versus 238 kJ mol^{-1} for the average of TS-2PZ and TS-2PE). Furthermore, the stability of the pre-reactive complex 1Z or 1E (ruling the barrierless entrance channel) and that of the intermediate 2 (involved in the two-step mechanism) are greater in the case of the addition of C_2H than for CN (−218.7 versus −203.6 kJ mol^{-1} for the average of 1Z,1E and −299.7 versus −284.6 kJ mol^{-1} for 2).

Moving to the attack to the N-end of methanimine, from the inspection of Figure 1, it is evident that the two possible paths originating from the 1N pre-reactive complex are similar to those described above for the C-end attack, as already noted for the CH_2NH+CN reaction (Vazart et al. 2015). With the only exception of 1N, which lies lower in energy than 1Z and 1E, all intermediates and transition states of these paths are less stable

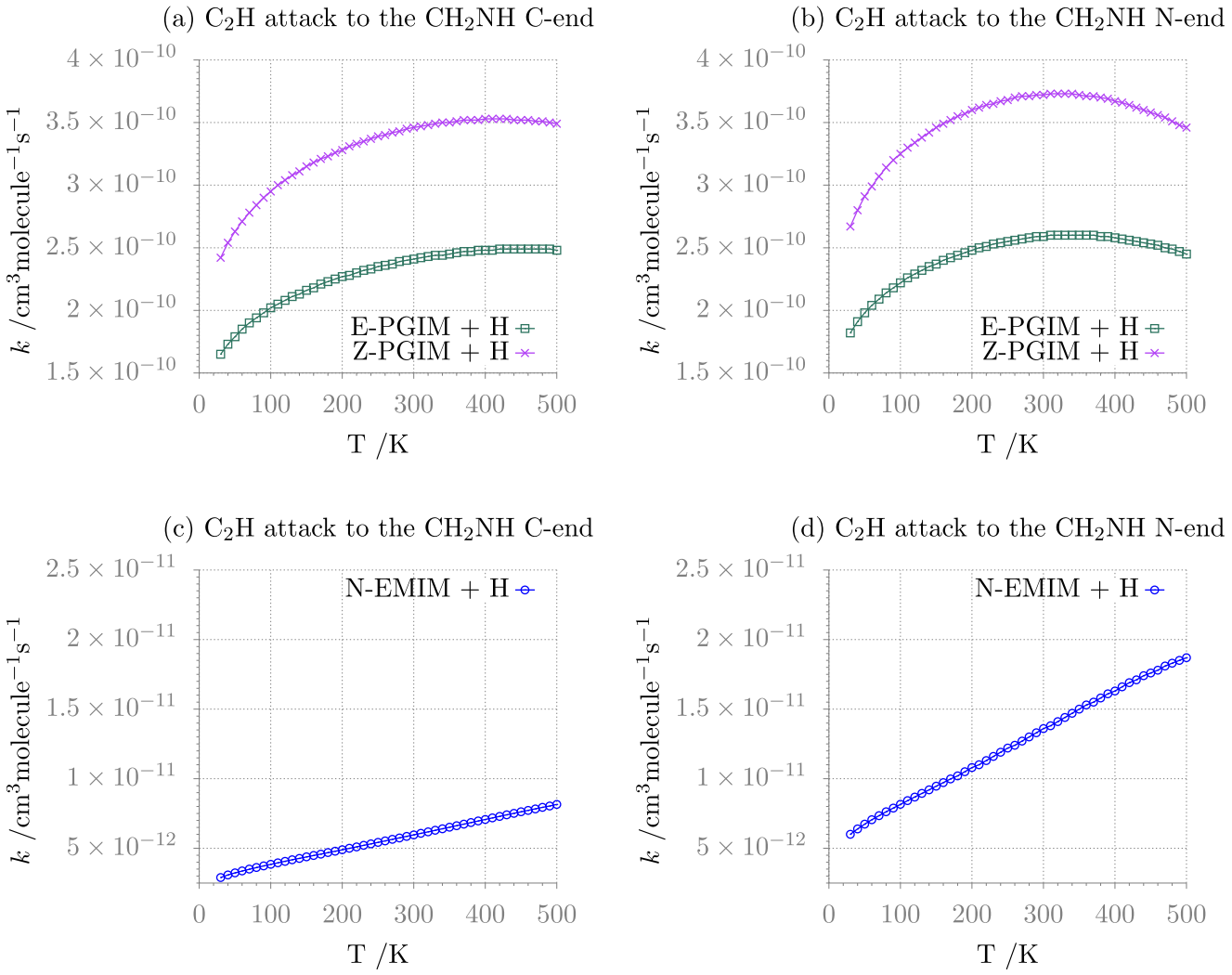

Figure 2. Temperature-dependence plots of the CH_2NH+C_2H reaction rate constants.

with respect to the C-end counterparts. The product itself, i.e., N-EMIM + H (PN), lies at higher energy: −72.7 kJ mol^{-1}, to be compared with −106.6 kJ mol^{-1} for E-PGIM + H (PE) and −110.0 kJ mol^{-1} for Z-PGIM + H (PZ).

Studies for reactions of radical species with molecules containing a double bond have shown that the reactivity depends on the type of system. For the C = C bond, addition/elimination is barrierless and strongly favored over hydrogen elimination (e.g., Bouwman et al. 2012), whereas for C = O bonds, only H elimination is barrierless, whereas both the C- and O- addition/eliminations involve small barriers (e.g., Dong et al. 2005). Preliminary computations for the addition of other radicals (e.g., CP, OH, and CH_3) to methanimine show that the mechanism described in the previous paragraphs for the reaction with C_2H or CN represents a quite general route to the formation of complex imines, although in a few cases (e.g., CH_3) some transition states are not submerged with respect to reactants.

3.2. Rate Constants

To definitely confirm the effectiveness of the mechanism proposed, kinetic computations are required. The product specific rate constants as a function of temperature are shown in Figure 2 for the reaction of methanimine with C_2H and in Figure 3 for the reaction with CN, whereas the parameters of the Arrhenius–Kooij fits are given in Table 2. These have been obtained by fitting the global rate constants computed in the 20–500 K range. In more detail, for each figure, four panels are provided: those on the left refer to the C-end attack (panels (a) and (c)), while those on the right to the N-end attack (panels (b) and (d)). In both figures, the top panels show the temperature profiles of rate constants for the formation of the "C-isomers" (namely, Z-/E-PGIM and Z-/E-C-cyanomethanimine, CMIM), while the bottom panels refer to the formation of the "N-isomers" (namely, N-EMIM and N-cyanomethanimine, N-CMIM).

Focusing on the C-end reaction paths, the prevalence of the Z-product is related to the slightly lower energy of the corresponding transition states compared to those leading to the E isomer. Back-dissociation into reactants is negligible in the whole temperature range considered, whereas the overall rate constant for the PGIM formation raises by increasing the temperature, also showing progressive deviations from the Arrhenius behavior. The overall rate constant, which is of the order of 2–3 × 10^{-10} cm^3 molecule^{-1} s^{-1}, is mainly ruled by the one-step mechanism leading to products from the 1Z/1E pre-reactive complex through the TS-1ZPZ/TS-1EPE transition state. However, this is always true for Z-PGIM, while for the E

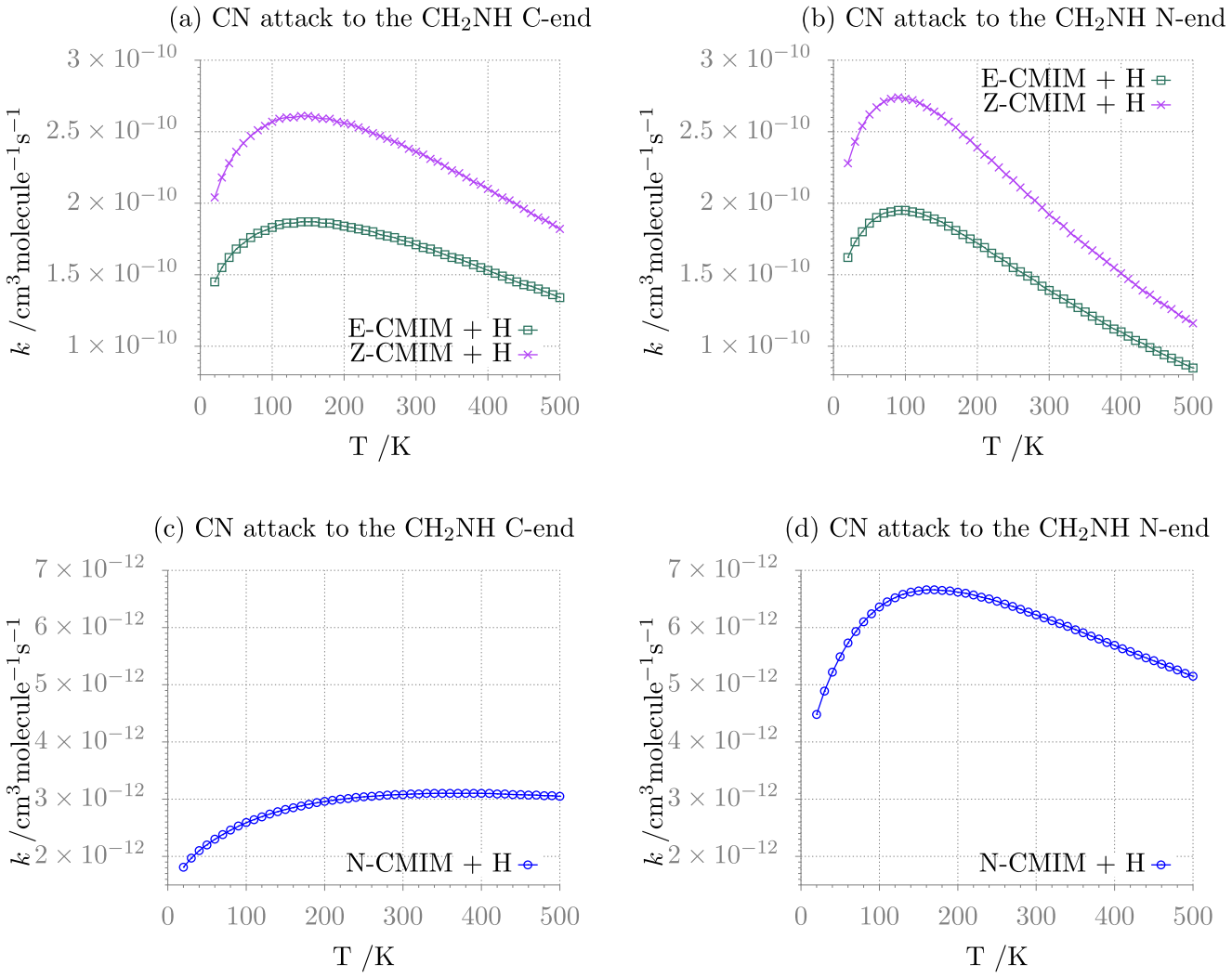

Figure 3. Temperature-dependence plots of the CH_2NH+CN reaction rate constants.

isomer the two-step mechanism seems to be the rate determining one above ∼350 K. The derived branching ratio is of the order of 1.5, smaller than the observational result (⩾1.9), as already noted in the case of C-cyanomethanimine. However, as in the latter case, the isomer abundance ratio obtained from astronomical observations is affected by a large uncertainty (the fractional abundance of E being indirectly derived), and it is, instead, close to the value obtained from a thermodynamic estimate based on the relative stability of the E and Z isomers. The considerations above on the computed isomers ratio assume a similar destruction rate for both E and Z species. In the case of C-cyanomethanimine, it has been suggested that the strong difference between the dipole moments of the E and Z forms (4.2 D and 1.4 D, respectively, from Vazart et al. 2015) leads to significantly different destruction rates (see Shingledecker et al. 2020). More specifically, Shingledecker et al. (2020) proposed a general rule-of-thumb for estimating the abundances of isomers based on their dipole moments, which has been denoted as "relative dipole principle." According to this, for propargylimine, whose isomers have very similar dipole moments (∼2 D, see Bizzocchi et al. 2020), the assumption that they have similar destruction rates seems to be reasonable. At the same time, different reaction rates with H radicals cannot be invoked since, for both cyanomethanimine and propargylimine, the corresponding reactions are ruled by non-submerged transition states. Further investigation of alternative mechanisms would be surely warranted, but it is out of the scope of the present Letter. As already noted for thermochemistry, the general kinetic features for the C_2H and CN additions to methanimine are very similar, thus giving further support to the plausibility and generality of the proposed mechanism. At 100 K, for PGIM, the overall rate constants for Z and E species (in cm^3 $molecule^{-1}$ s^{-1}) are 3.25×10^{-10} and 2.22×10^{-10}, respectively, to be compared to 2.73×10^{-10} and 1.95×10^{-10} for the two corresponding isomers of C-cyanomethanimine.

As far as the formation of the N-species is concerned, it is interesting to note that this process would be a little bit favored over formation of the C-species if the attacks to the two ends of the imino group would be independent (as actually is in the case of the CN addition to the CH_3 or NH_2 moiety of methylamine; see Puzzarini et al. 2020, with a rate constant of 4–5 $\times$ 10^{-10} cm^3 $molecule^{-1}$ s^{-1}). However, Figure 1 shows that the two channels are connected by a low-lying cyclic intermediate. Under these circumstances (also valid for the attack of the CN radical), the formation of C-products becomes faster by two orders of magnitude with respect to formation of the N-product, with the rate constant of the latter process slightly increasing with the temperature. To provide a graphical

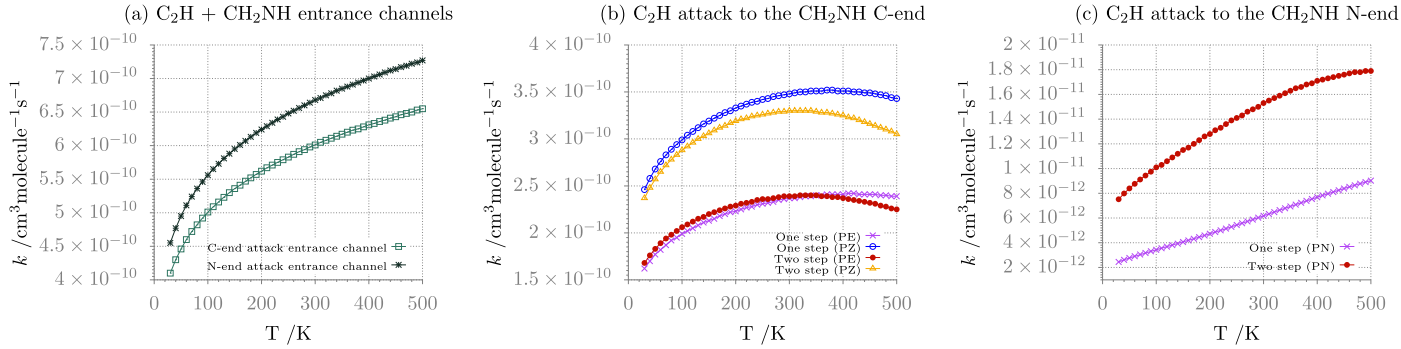

Figure 4. Temperature dependence of the rate constants for the elementary steps of the overall CH_2NH+C_2H reaction, namely barrierless entrance (panel (a)), and one- or two-step paths leading to Z-/E-PGIM (panel (b)) and N-EMIM (panel (c)).

Table 2
The Arrhenius–Kooij Parameters for the CH_2NH+X Reaction

	C-end Attack			N-end Attack		
X = C_2H	E	Z	N	E	Z	N
A/cm^3 molecule^{-1} s^{-1}	2.43×10^{-10}	3.51×10^{-10}	5.54×10^{-12}	2.66×10^{-10}	3.83×10^{-10}	1.26×10^{-11}
n	7.58×10^{-2}	3.86×10^{-2}	6.33×10^{-1}	-6.10×10^{-2}	-9.22×10^{-2}	6.59×10^{-1}
E/kJ mol^{-1}	6.74×10^{-2}	8.72×10^{-2}	-2.32×10^{-1}	1.62×10^{-1}	1.77×10^{-1}	-2.15×10^{-1}
rms[a]	4.37×10^{-12}	7.12×10^{-12}	1.15×10^{-13}	1.02×10^{-11}	1.54×10^{-11}	1.97×10^{-13}
X = CN	E	Z	N	E	Z	N
A/cm^3 molecule^{-1} s^{-1}	1.75×10^{-10}	2.42×10^{-10}	3.12×10^{-12}	1.46×10^{-10}	2.03×10^{-10}	6.51×10^{-12}
n	-3.20×10^{-1}	-3.40×10^{-1}	2.68×10^{-2}	-6.56×10^{-1}	-6.68×10^{-1}	-2.72×10^{-1}
E/ kJ mol^{-1}	2.17×10^{-1}	2.24×10^{-1}	1.03×10^{-1}	3.37×10^{-1}	3.39×10^{-1}	2.33×10^{-1}
rms[a]	1.09×10^{-11}	1.55×10^{-11}	8.39×10^{-14}	1.47×10^{-11}	2.07×10^{-11}	3.29×10^{-13}

Note.
[a] rms stands for root-mean-square deviation of the fit.

explanation of the behavior of the global constant with temperature, the contributions of some specific reaction channels are shown in Figure 4. These are the two barrierless (C- and N-end) entrance channels, the one- and two-step processes leading to Z-/E-PGIM for the C-end attack and the corresponding channel leading to N-EMIM for the attack to the N end of methanimine. It is noted that, even if the entrance channel flux for the N-end attack is faster than the C-end attack one, the subsequent high barriers of the N-EMIM formation path slow down the flux, thus resulting in the preferential formation of the E,Z-PGIM, which presents lower lying barriers. In this picture, an important role is played by the TS-CY-N transition state linking 1N to the cyclic pre-reactive complex, CYCLO-1. In fact, this interconversion is the elementary step characterized by the lowest barrier for the N-end side of the overall CH_2NH+C_2H reaction. Similar arguments also apply to the reaction involving CN.

It is noteworthy that the behavior discussed above for both types of radical attack to methanimine is specific of the low pressure limit (see computational details). In fact, moving to a pressure of 1 atm (of limited astrophysical interest, but of potential relevance in planetary atmospheres), the N-EMIM formation remains unfavorable with respect to E,Z-PGIM but all formation rate constants become slower. This trend is due to the stabilization of the entrance channel wells (namely 1N and 1Z) by collisions (that occurs at pressure values as high as 1 atm), thus leading to an increase of the effective reaction barriers with the consequent decrease of the overall rate constant, which shows a monotonic increase with temperature.

A curved Arrhenius plot is obtained when the activation energy depends on the temperature and this behavior is captured by the Arrhenius–Kooij formula (see Equation (1)) when this dependence is linear. The rms deviations reported in Table 2 demonstrate that the data for the C_3H_3N imine isomers are indeed well fitted by the Arrhenius–Kooij expression. Within this model, E represents the activation energy at 0 K and the activation energy at a generic temperature T is given by $E + n\left(\frac{RT}{300}\right)$. In the present case, the activation energy is always positive, with the exception of N-EMIM, as a result of both the capture rate constant and the subsequent energy barriers for the unimolecular steps. The n parameter (the first derivative of the activation energy with respect to temperature) is always positive for the C-end attack, while it is negative for the PGIM isomers when the N-end attack takes place. Finally, the values of the pre-exponential factor A are typical for this kind of reactions and rule the branching ratio between the Z and E PGIM isomers. Indeed, the ratio of the A factors is 1.44 and the branching ratio ranges between 1.43 and 1.47 in the whole temperature range (20–500 K).

4. Concluding Remarks

In this Letter, we have proposed a gas-phase formation route for the recently detected Z-PGIM molecule. In analogy to the addition of the CN radical to methanimine leading to cyanomethanimine,

addition of the isoelectronic ethynyl radical easily leads to PGIM through a similar reaction mechanism, which involves the formation of a stable pre-reactive complex and its successive evolution by means of submerged transition states. Since the level of the QC and kinetic computations carried out gives strong supports to the quantitative accuracy of our results, search for PGIM isomers in the other regions of the ISM where methanimine and the ethynyl radical have been both detected could be attempted to further validate the proposed reaction mechanism.

In a more general perspective, the results of our state-of-the-art computations provide convincing evidences about the feasibility of a general addition/elimination mechanism for the formation of complex imines. This starts from methanimine as a precursor and involves reactive radicals abundantly present in the interstellar space.

This work has been supported by MIUR (grant No. 2017A4XRCA) and by the University of Bologna (RFO funds). The SMART@SNS Laboratory (http://smart.sns.it) is acknowledged for providing high-performance computing facilities. Support by the Italian Space Agency (ASI; "Life in Space" project, No. 2019-3-U.0) is also acknowledged.

ORCID iDs

Jacopo Lupi https://orcid.org/0000-0001-6522-9947
Cristina Puzzarini https://orcid.org/0000-0002-2395-8532
Vincenzo Barone https://orcid.org/0000-0001-6420-4107

References

Baiano, C., Lupi, J., Tasinato, N., Puzzarini, C., & Barone, V. 2020, Molecules, 25, 2873
Bizzocchi, L., Prudenzano, D., Rivilla, V. M., et al. 2020, A&A, 640, A98
Bloino, J., Biczysko, M., & Barone, V. 2012, J. Chem. Theory Comp., 8, 1015
Bouwman, J., Goulay, F., Leone, S. R., & Wilson, K. R. 2012, JPCA, 116, 3907
Bowman, M. C., Burke, A. D., Turney, J. M., & Schaefer, H. F., III 2020, MolPh, 118, e1769214
Chesnavich, W. J. 1986, JChPh, 84, 2615
Codella, C., Ceccarelli, C., Caselli, P., et al. 2017, A&A, 605, L3
Curtiss, L. A., Redfern, P. C., & Raghavachari, K. 2007, JChPh, 126, 084108
Dickens, J. E., Irvine, W. M., DeVries, C. H., & Ohishi, M. 1997, ApJ, 479, 307
Dong, H., Ding, Y.-h., & Sun, C.-c. 2005, JChPh, 122, 204321
Dunning, T. H., Jr. 1989, JChPh, 90, 1007
Eckart, C. 1930, PhRv, 35, 1303
Fernández-Ramos, A., Miller, J. A., Klippenstein, S. J., & Truhlar, D. G. 2006, ChRv, 106, 4518
Frisch, M. J., Trucks, G. W., Schlegel, H. B., et al. 2016, Gaussian 16 Revision C.01
Georgievskii, Y., Miller, J. A., Burke, M. P., & Klippenstein, S. J. 2013, JPCA, 117, 12146
Godfrey, P. D., Brown, R. D., Robinson, B. J., & Sinclair, M. W. 1973, ApL, 13, 119
Grimme, S. 2006, JChPh, 124, 034108
Grimme, S., Antony, J., Ehrlich, S., & Krieg, H. 2010, JChPh, 132, 154104
Grimme, S., Ehrlich, S., & Goerigk, L. 2011, JCoCh, 32, 1456
Helgaker, T., Klopper, W., Koch, H., & Noga, J. 1997, JChPh, 106, 9639
Herbst, E., & van Dishoeck, E. F. 2009, ARA&A, 47, 427
Kawaguchi, K., Takano, S., Ohishi, M., et al. 1992, ApJL, 396, L49
Kooij, D. 1893, Zeitschr. Phys. Chem., 12, 155
Krim, L., Guillemin, J. C., & Woon, D. E. 2019, MNRAS, 485, 5210
Laidler, K. J. 1996, PApCh, 68, 149
Loomis, R. A., Zaleski, D. P., Steber, A. L., et al. 2013, ApJL, 765, L9
Lovas, F. J., Hollis, J. M., Remijan, A. J., & Jewell, P. R. 2006, ApJL, 645, L137
Lupi, J., Puzzarini, C., Cavallotti, C., & Barone, V. 2020, J. Chem. Theory Comp., 16, 5090
McGuire, B. A. 2018, ApJS, 239, 17
Møller, C., & Plesset, M. S. 1934, PhRv, 46, 618
Montgomery, J. A., Frisch, M. J., Ochterski, J. W., & Petersson, G. A. 2000, JChPh, 112, 6532
Papajak, E., Zheng, J., Xu, X., Leverentz, H. R., & Truhlar, D. G. 2011, J. Chem. Theory Comp., 7, 3027
Pechukas, P., & Light, J. C. 1965, JChPh, 42, 3281
Puzzarini, C., & Barone, V. 2011, PCCP, 13, 7180
Puzzarini, C., & Barone, V. 2020, PCCP, 22, 6507
Puzzarini, C., Biczysko, M., Barone, V., et al. 2014, J. Phys. Chem. Lett., 5, 534
Puzzarini, C., Bloino, J., Tasinato, N., & Barone, V. 2019, ChRv, 119, 8131
Puzzarini, C., Salta, Z., Tasinato, N., et al. 2020, MNRAS, 496, 4298
Raghavachari, K., Trucks, G. W., Pople, J. A., & Head-Gordon, M. 1989, CPL, 157, 479
Rivilla, V. M., Martín-Pintado, J., Jiménez-Serra, I., et al. 2018, MNRAS, 483, L114
Salta, Z., Tasinato, N., Lupi, J., et al. 2020, ESC, 4, 774
Shingledecker, C. N., Molpeceres, G., Rivilla, V. M., Majumdar, L., & Kästner, J. 2020, ApJ, 897, 158
Theule, P., Borget, F., & Mispelaer, F. e. a. 2011, A&A, 534, A64
Tonolo, F., Lupi, J., Puzzarini, C., & Barone, V. 2020, ApJ, 900, 85
Vazart, F., Calderini, D., Puzzarini, C., Skouteris, D., & Barone, V. 2016, J. Chem. Theory Comp., 12, 5385
Vazart, F., Latouche, C., Skouteris, D., Balucani, N., & Barone, V. 2015, ApJ, 810, 111
Woon, D. E., & Dunning, T. H., Jr. 1995, JChPh, 103, 4572
Zaleski, D. P., Seifert, N. A., Steber, A. L., et al. 2013, ApJL, 765, L10
Zeng, S., Jiménez-Serra, I., Rivilla, V. M., et al. 2018, MNRAS, 478, 2962